

Testing Conditional Mean Independence Using Generative Neural Networks

Yi Zhang*, Linjun Huang*, Yun Yang and Xiaofeng Shao [†]

January 30, 2025

Abstract

Conditional mean independence (CMI) testing is crucial for statistical tasks including model determination and variable importance evaluation. In this work, we introduce a novel population CMI measure and a bootstrap-based testing procedure that utilizes deep generative neural networks to estimate the conditional mean functions involved in the population measure. The test statistic is thoughtfully constructed to ensure that even slowly decaying nonparametric estimation errors do not affect the asymptotic accuracy of the test. Our approach demonstrates strong empirical performance in scenarios with high-dimensional covariates and response variable, can handle multivariate responses, and maintains nontrivial power against local alternatives outside an $n^{-1/2}$ neighborhood of the null hypothesis. We also use numerical simulations and real-world imaging data applications to highlight the efficacy and versatility of our testing procedure.

Keywords: Conditional Distribution, Maximum Mean Discrepancy, Kernel Method, Double Robustness.

*Equal contribution

[†]Yi Zhang and Linjun Huang are Ph.D. students at Department of Statistics, University of Illinois at Urbana-Champaign, Champaign, USA. Yun Yang is Associate Professor at Department of Mathematics, University of Maryland, College Park MD, USA. Xiaofeng Shao is Professor at Department of Statistics and Data Science, Washington University in St Louis, USA. Emails: yiz19@illinois.edu, linjunh2@illinois.edu, yy84@umd.edu and shaox@wustl.edu.

1 Introduction

Conditional mean independence (CMI) testing is a fundamental tool for model simplification and assessing variable importance, and plays a crucial role in statistics and machine learning. In traditional statistical applications, such as nonparametric regression, CMI testing identifies subsets or functions of covariates that meaningfully predict the response variable. This is essential for improving model efficiency, accuracy, and interpretability by avoiding redundant variables. In machine learning, CMI testing has broad applications in areas like interpretable machine learning (Murdoch et al., 2019), representation learning (Bengio et al., 2013; Huang et al., 2024) and transfer learning (Maqsood et al., 2019; Zhuang et al., 2020).

In this paper, we address the problem of CMI testing for multivariate response variables and covariates. Specifically, for random vectors $X \in \mathbb{R}^{d_x}$, $Y \in \mathbb{R}^{d_y}$, and $Z \in \mathbb{R}^{d_z}$, we test the null hypothesis H_0 that Y is conditionally mean independent of X given Z , i.e., $\mathbb{E}[Y|X = x, Z = z] = \mathbb{E}[Y|Z = z]$, a.e. $(x, z) \in \mathbb{R}^{d_x+d_z}$. For example, consider predicting age Y from a facial image. To test whether Y can be predicted using images with a specific facial region (potentially containing sensitive information) covered in black, X can represent the covered region and Z the remaining facial image. Similarly, to test whether Y can be predicted using a low-resolution version or extracted features of a facial image, X can represent the original image and Z a low-dimensional feature vector derived from X using standard extraction methods (e.g., Autoencoder, Average pooling, or PCA (Berahmand et al., 2024)). Under H_0 , removing X from the predictive model $f(X, Z)$, where $f : \mathbb{R}^{d_x+d_z} \rightarrow \mathbb{R}^{d_y}$ denotes the nonparametric regression function, does not reduce prediction accuracy.

For machine learning tasks, identifying which (functions of) covariates contribute to predicting the response is particularly important, as deep neural networks (DNNs) often process high-dimensional data, such as images and text, that may include irrelevant features (Li et al., 2017; Van Landeghem et al., 2010). Performing dimensionality reduction before DNN training provides several advantages: it enhances interpretability, improves prediction accuracy, and reduces computational costs (Cai et al., 2018). In evaluating DNN training, covariate significance is typically assessed by comparing performance metrics, such as mean squared error or classification accuracy, for DNNs trained with and without specific covariates (Dai et al., 2022; Williamson et al., 2023). As discussed in Section 2.3 of Williamson et al. (2023), many common performance metrics, such as the coefficient of determination (R^2) for regression and empirical risk with cross-entropy or 0-1 loss for binary classification, are functionals of the conditional mean functions of Y , which means H_0 will imply that the covariates are not significant. Thus, CMI testing provides a valuable tool for assessing covariate importance across a variety of machine learning applications.

1.1 Related literature

To the best of our knowledge, most existing CMI tests focus on univariate Y and face one or more of the following three major issues: (1) finite-sample performance deteriorates when some or all of (X, Y, Z) are high-dimensional; (2) the tests lack theoretical size guarantees in general nonparametric settings; and (3) they exhibit weak power in detecting local alternatives. For a recent survey, see Lundborg (2022). We discuss how these challenges arise and how existing CMI tests have partially addressed them.

Performance deterioration in high dimensional setting. This issue primarily arises from the estimation of the conditional mean functions $r(z) := \mathbb{E}[Y|Z = z]$ and $m(x, z) := \mathbb{E}[Y|X = x, Z = z]$.

Early CMI tests, such as those in Fan and Li (1996); Delgado and Manteiga (2001); Zhu and Zhu (2018); Lavergne and Vuong (2000); Ait-Sahalia et al. (2001), relied on kernel smoothing methods for these estimations. Consequently, these CMI tests suffer from the curse of dimensionality: their performance declines significantly as the dimensions d_Z , $d_X + d_Z$, and/or d_Y increase (Zhou et al., 2022, Section 1). For instance, Figure 1 in Zhu and Zhu (2018) shows that the empirical power of tests proposed by Fan and Li (1996) and Delgado and Manteiga (2001) decreases sharply with increasing d_Z and d_X , exhibiting trivial power under a sample size of $n = 200$ with moderate dimensionality ($d_Z = 4$ and $d_X \geq 8$). To address this, recent CMI tests utilize machine learning tools, such as deep neural networks (DNNs) and the kernel trick, to estimate conditional mean functions. These tools are effective in approximating complex, high-dimensional functions with underlying low-dimensional structures. For example, tests in Williamson et al. (2021); Dai et al. (2022); Lundborg et al. (2024); Cai et al. (2022); Williamson et al. (2023); Cai et al. (2024) leverage DNNs for conditional mean estimation, achieving better performance in high-dimensional settings.

Theoretical size guarantee. The main challenge in establishing a theoretical size guarantee stems from two key issues. First, most of the existing CMI tests (except the one proposed by Delgado and Manteiga (2001)) rely on the sample estimation of the population CMI measure $\Gamma := \mathbb{E}[(r(Z) - m(X, Z))^2 w(X, Z)]$ or its equivalent forms, where w is a positive weight function. A common plug-in estimator of Γ is given by $\hat{\Gamma}(\hat{r}, \hat{m}) = n^{-1} \sum_{i=1}^n (\hat{r}(Z_i) - \hat{m}(X_i, Z_i))^2 w(X_i, Z_i)$, where \hat{r} and \hat{m} are estimators of the conditional mean functions. For a population CMI measure to be valid, it must uniquely characterize CMI, meaning that the measure equals zero if and only if H_0 holds. While Γ satisfies this requirement, its estimator $\hat{\Gamma}(\hat{r}, \hat{m})$ suffers from a degeneracy problem: under H_0 , $\hat{\Gamma}(\hat{r}, \hat{m})$ converges to zero at a rate faster than the $n^{-1/2}$ rate at which $\hat{\Gamma}(r, m) - \Gamma$ converges to a non-degenerate limiting distribution under the alternative (Fan and Li, 1996, Section 1).

Second, the nonparametric estimation errors for $r(z)$ and $m(x, z)$ typically decay slower than the $n^{-1/2}$ parametric rate, and the convergence rate of $\hat{\Gamma}(\hat{r}, \hat{m})$ under H_0 depends heavily on how quickly these errors decay. For CMI tests that use kernel smoothing to estimate the conditional mean functions, the estimation error has an explicit form, allowing it to be addressed directly, along with the degeneracy issue, when deriving asymptotic results under H_0 . As a result, all the aforementioned kernel smoothing-based CMI tests have theoretical size guarantees. In contrast, due to the black-box nature of DNNs, the estimation errors for $r(z)$ and $m(x, z)$ cannot be explicitly decomposed or handled in the same way as kernel smoothing estimators. Consequently, addressing the degeneracy issue requires additional debiasing procedures to mitigate the impact of these errors and achieve accurate size control. For example, Williamson et al. (2021) and Lundborg et al. (2024) constructed statistics based on alternative forms of Γ to reduce bias. However, the degeneracy issue persists: as shown in Theorem 1 of Williamson et al. (2021), their estimator is \sqrt{n} -consistent when $\Gamma > 0$, but no asymptotic results are provided under H_0 (i.e., $\Gamma = 0$). Similarly, the test in Lundborg et al. (2024), which builds on the conditional independence test from Shah and Peters (2020), relies on strong assumptions to bypass the degeneracy issue, as outlined in Section 2.1 and Part (a) of Theorem 4 in Lundborg et al. (2024). To address the degeneracy issue, Dai et al. (2022) introduced additional noise of order $O_p(n^{-1/2})$ to the estimator of Γ , while Williamson et al. (2023) utilized sample splitting to estimate separate components of an equivalent form of Γ on different subsamples. However, both approaches are ad hoc (Section 6.2 of Verdinelli and Wasserman (2024)) and, as discussed in Appendix S3 of Lundborg et al. (2024), suffer from significant power loss under the alternative hypothesis.

Weak power against local alternatives. On one hand, the CMI tests proposed in Fan and Li

Table 1: Summary of existing CMI tests. **High-Dim**: whether the test has good empirical performance when some or all the dimensions of X , Y and Z are large; **Size Guarantee**: whether the test has theoretical results under H_0 that guarantee accurate asymptotic size control in general nonparametric setting; **Local Alt**: whether the test can detect local alternatives with signal strength Δ_n converging to zero at the parametric rate $n^{-1/2}$.

Tests	High-Dim	Size Guarantee	Local Alt
Fan and Li (1996)	No	Yes	No
Delgado and Manteiga (2001)	No	Yes	Yes
Zhu and Zhu (2018)	No	Yes	No
Lavergne and Vuong (2000)	No	Yes	No
Ait-Sahalia et al. (2001)	No	Yes	No
Williamson et al. (2021)	Yes	No	No
Dai et al. (2022)	Yes	Yes	No
Lundborg et al. (2024)	Yes	No	Yes
Williamson et al. (2023)	Yes	Yes	No
Cai et al. (2024)	Yes	Yes	No
Our method	Yes	Yes	Yes

(1996); Zhu and Zhu (2018); Lavergne and Vuong (2000); Ait-Sahalia et al. (2001); Williamson et al. (2021); Dai et al. (2022); Williamson et al. (2023) fail to detect local alternatives with signal strength $\Delta_n := \sqrt{\mathbb{E}[(r(Z) - m(X, Z))^2]}$ of order $n^{-1/2}$, primarily due to their reliance on the population measure Γ . Specifically, the tests in Fan and Li (1996); Zhu and Zhu (2018); Lavergne and Vuong (2000); Ait-Sahalia et al. (2001) take the form $nh^{s/2}\hat{\Gamma}$, where $h \rightarrow 0$ is a bandwidth parameter used in kernel smoothing, and $s = d_Z$ or $d_X + d_Z$. Consequently, these tests cannot detect local alternatives converging to the null faster than $n^{-1/2}h^{-s/4}$. The tests in Williamson et al. (2021); Dai et al. (2022); Williamson et al. (2023) use the population CMI measure $\Gamma_0 = \Gamma_1 - \Gamma_2$, where $\Gamma_1 = \mathbb{E}[(Y - r(Z))^2]$ and $\Gamma_2 = \mathbb{E}[(Y - m(X, Z))^2]$, which is equivalent to Γ . Since the quadratic terms Γ_1 and Γ_2 can only be estimated at the $n^{-1/2}$ rate, these tests are limited to detecting local alternatives with Δ_n of order $n^{-1/4}$. On the other hand, the test proposed in Cai et al. (2024) employs sample splitting and requires the size of the training subsample used to estimate the conditional mean functions to be substantially larger than that of the testing subsample. As a result, their test is limited to detecting local alternatives with Δ_n converging to zero slower than $n^{-1/2}$, which can still result in significant power loss in practice.

1.2 Our contributions

Table 1 summarizes limitations of existing CMI tests. To overcome these challenges, we propose a novel CMI testing procedure with the following advantages:

1. The test demonstrates strong empirical performance even when some or all dimensions of X , Y , and Z are high. Notably, it is well-suited for scenarios where imaging data serve as covariates, responses, or both.
2. The test achieves precise asymptotic size control under H_0 .
3. The test exhibits nontrivial power against local alternatives outside an $n^{-1/2}$ -neighborhood of H_0 .

To achieve these features, we propose a new population CMI measure closely related to the conditional independence measure introduced in Daudin (1980). Additionally, we develop a sample version of this population measure in a multiplicative form, which is key to mitigating the impact of estimation errors in nonparametric nuisance parameters (i.e., the conditional mean functions). Our test not only requires estimating $r(z)$ but also the conditional mean embedding (CME, Song

et al., 2009, Definition 3) of X given Z into a reproducing kernel Hilbert space (RKHS) on the space of X . Instead of directly estimating the CME using DNNs, we train a generative neural network (GNN) to sample from the (approximated) conditional distribution of X given Z . The CME is then estimated using the Monte Carlo method with samples generated from the trained GNN.

1.3 Organization and notations

The paper is organized as follows: Section 2 introduces the proposed population CMI measure, the test statistic, and the bootstrap calibration procedure, along with its asymptotic properties and consistency results. Section 3 evaluates the test using finite sample simulations, comparing it with other methods. Section 4 presents two real data examples. Section 5 concludes with final remarks. All proofs and additional details are deferred to the Appendix.

The following notations will be used throughout the paper. For any positive integer d and random vectors $(X^1, X^2, \dots, X^d, Z)$ defined on the same probability space, $\mathbb{P}_{X^1 X^2 \dots X^d}$ and $\mathbb{P}_{X^1 X^2 \dots X^d | Z}$ denote the joint distribution of X^1, X^2, \dots, X^d and its conditional distribution given Z , respectively. Let \mathbb{E}_Z represent the expectation with respect to \mathbb{P}_Z , and let \mathbb{P}_m denote the Lebesgue measure on \mathbb{R}^d . For a positive integer n , define $[n] = \{1, 2, \dots, n\}$. For a probability measure $\mu(\cdot)$ on \mathbb{R}^d and $p \geq 1$, let $L_p(\mathbb{R}^d, \mu) = \{f : \mathbb{R}^d \rightarrow \mathbb{R} : \int |f(x)|^p d\mu(x) < \infty\}$. For any Hilbert spaces A and B , let $A \otimes B$ denote their tensor product, and use $\langle \cdot, \cdot \rangle_A$ and $\|\cdot\|_A$ to denote the inner product and induced norm on A , respectively. For random vectors $a, b \in \mathbb{R}^d$, the Gaussian kernel is defined as $\mathcal{K}(a, b) = \exp(-\|a - b\|_2^2 / (2\sigma^2))$ and the Laplacian kernel as $\mathcal{K}(a, b) = \exp(-\|a - b\|_1 / \sigma)$, where $\sigma > 0$ is the bandwidth parameter, $\|\cdot\|_2$ is the Euclidean ℓ_2 -norm, and $\|\cdot\|_1$ is the ℓ_1 -norm.

2 Conditional Mean Independence Testing

In this section, we introduce a novel population measure for evaluating CMI and propose a corresponding sample-based statistic for conducting the CMI test. We then establish theoretical guarantees for the proposed procedure, including size control and power against local alternatives.

2.1 Population conditional mean independence measure

Recall that the goal is to test the null hypothesis of $H_0 : \mathbb{E}[Y|X, Z] = \mathbb{E}[Y|Z]$ a.s.- \mathbb{P}_{XZ} against the alternative hypothesis of $H_1 : \mathbb{P}(\mathbb{E}[Y|X, Z] \neq \mathbb{E}[Y|Z]) > 0$. To motivate our population measure for evaluating CMI, we begin with the following result, which provides equivalent characterizations of CMI (Daudin, 1980).

Proposition 1. *If $\mathbb{E}[\|Y\|_2^2] < \infty$, then the following properties are equivalent to each other:*

- (a) $\mathbb{E}[Y|X, Z] = \mathbb{E}[Y|Z]$ a.s.- \mathbb{P}_{XZ} .
- (b) $\mathbb{E}[(f(X, Z) - \mathbb{E}[f(X, Z)|Z])Y] = 0$ for any $f \in L_2(\mathbb{R}^{d_X+d_Z}, \mathbb{P}_{XZ})$.
- (c) $\mathbb{E}[(f(X, Z) - \mathbb{E}[f(X, Z)|Z])(Y - \mathbb{E}[Y|Z])] = 0$ for any $f \in L_2(\mathbb{R}^{d_X+d_Z}, \mathbb{P}_{XZ})$.

Remark 2. It is straightforward to see that (a) \Rightarrow (b) \Rightarrow (c), and (c) implies (a) by taking $f(X, Z) = \mathbb{E}[Y^\top c | X, Z]$ over all $c \in \mathbb{R}^{d_Y}$. The only difference between (c) and (b) in Proposition 1 is that Y is centered at $\mathbb{E}[Y|Z]$ in (c). This additional centering is crucial for reducing biases from the estimation of the conditional mean functions; our proposed population CMI measure will be derived from (c) by considering all f within a dense subset of $L_2(\mathbb{R}^{d_X+d_Z}, \mathbb{P}_{XZ})$.

Let $\mathcal{K}_X : \mathbb{R}^{d_X} \times \mathbb{R}^{d_X}$ and $\mathcal{K}_Z : \mathbb{R}^{d_Z} \times \mathbb{R}^{d_Z}$ denote two symmetric positive-definite kernel functions that define two reproducing kernel Hilbert spaces (RKHS) \mathbb{H}_X and \mathbb{H}_Z over the spaces of X and Z , respectively. Additionally, let $\mathcal{K}_0 = \mathcal{K}_X \times \mathcal{K}_Z$ represent the product kernel, with \mathbb{H}_0 being the corresponding RKHS induced by \mathcal{K}_0 over the product space $\mathbb{R}^{d_X} \times \mathbb{R}^{d_Z}$. Motivated by part (c) of Proposition 1, we define linear operator $\Sigma : \mathbb{R}^{d_Y} \rightarrow \mathbb{H}_0$,

$$\Sigma c = \mathbb{E} \left\{ \left[\mathcal{K}_0((X, Z), \cdot) - \mathbb{E}[\mathcal{K}_0((X, Z), \cdot) | Z] \right] \left[Y - \mathbb{E}[Y | Z] \right]^\top c \right\}, \quad \text{for any } c \in \mathbb{R}^{d_Y}.$$

From the reproducing property, we see that for any $f \in \mathbb{H}_0$ and any $c \in \mathbb{R}^{d_Y}$,

$$\langle f, \Sigma c \rangle_{\mathbb{H}_0} = \mathbb{E} \left\{ [f(X, Z) - \mathbb{E}[f(X, Z) | Z]] [Y - \mathbb{E}[Y | Z]]^\top c \right\}.$$

Under the assumption that the RKHS \mathbb{H}_0 is dense in $L_2(\mathbb{R}^{d_X+d_Z}, P_{XZ})$, which holds if \mathcal{K}_X and \mathcal{K}_Z are L_2 - or c_0 -universal kernels (Szabó and Sriperumbudur, 2018, Theorem 5), such as the Gaussian and Laplacian kernels considered in this paper, the preceding display along with Proposition 1 implies that the null hypothesis H_0 holds if and only if Σ is the zero operator (i.e., $\Sigma c = 0 \in \mathbb{H}_0$ for any $c \in \mathbb{R}^{d_Y}$). The following proposition formalizes this intuition and serves as the foundation for our proposed population CMI measure,

$$\begin{aligned} \Gamma^* &= \mathbb{E}[U(X, X') V(Y, Y') \mathcal{K}_Z(Z, Z')], \\ \text{where } V(Y, Y') &= [Y - g_Y(Z)]^\top [Y' - g_Y(Z')], \text{ and} \\ U(X, X') &= \mathcal{K}_X(X, X') - \langle g_X(Z), \mathcal{K}_X(X', \cdot) \rangle_{\mathbb{H}_X} \\ &\quad - \langle g_X(Z'), \mathcal{K}_X(X, \cdot) \rangle_{\mathbb{H}_X} + \langle g_X(Z), g_X(Z') \rangle_{\mathbb{H}_X}. \end{aligned} \tag{1}$$

Here, (X', Y', Z') is an independent copy of (X, Y, Z) , g_Y and g_X are defined as $g_Y(\cdot) = \mathbb{E}[Y | Z = \cdot] \in \mathbb{R}^{d_Y}$ and $g_X(\cdot) = \mathbb{E}[\mathcal{K}_X(X, \cdot) | Z = \cdot] \in \mathbb{H}_X$, respectively.

Proposition 3. *If Assumption 4(a) holds, then*

- (a) Σ is a Hilbert-Schmidt operator, and its Hilbert-Schmidt norm, denoted as $\|\Sigma\|_{\text{HS}}$, satisfies $\|\Sigma\|_{\text{HS}}^2 = \Gamma^*$.
- (b) The null H_0 holds if and only if $\Gamma^* = 0$.

Due to the multiplicative form inside the expectation in equation (1), when constructing a sample version of Γ^* as the test statistic, the estimation errors of the two nuisance parameters (g_X and g_Y) do not affect the asymptotic properties of the statistic, as long as the product of these errors decays faster than $n^{-1/2}$. This desirable property is commonly referred to as double robustness (Bang and Robins, 2005; Zhang et al., 2024).

Our Γ^* bears similarity to the maximum mean discrepancy-based conditional independence measure (MMDCI) proposed in Zhang et al. (2024), which was designed for testing the stronger null hypothesis of conditional independence (CI). While CI assumes that the conditional distribution of the response variable Y is independent of an additional covariate X given an existing covariate Z , the CMI assumption only requires that the conditional mean function of Y does not depend on X given Z . This means that including X in the regression function of Y does not improve its predictive ability in the mean squared error sense. In contrast, rejecting CI does not provide a direct interpretation in terms of predictive ability (Lundborg et al., 2024, Section 1). Furthermore, the MMDCI statistic compares the joint distribution of (X, Y, Z) under the null with its true distribution using maximum mean discrepancy (MMD) (Gretton et al., 2012), requiring stronger

assumptions to fully characterize CI (see Assumption 1 in Zhang et al. (2024)). In contrast, our population CMI measure avoids using MMD to capture the full distributional properties of (X, Y, Z) , making it more suitable for CMI testing compared to existing population CMI measures. Computationally, the test proposed in Zhang et al. (2024) requires training two generative neural networks (GNNs) to sample from the conditional distributions of X and Y given Z , respectively. In contrast, our proposed test statistic only requires sampling from the conditional distribution of X given Z , resulting in lower computational cost and reduced memory usage.

2.2 Testing procedure

To construct a sample version of Γ^* , it is necessary to estimate g_Y and g_X . To address the curse of dimensionality, we use deep neural networks (DNNs) to estimate g_Y . For g_X , which is an RKHS-valued function, we estimate $g_X(z)$ for a fixed $z \in \mathbb{R}^{dz}$ by sampling M copies $\{X_{z,i}\}_{i=1}^M$ from the conditional distribution of X given $Z = z$. The estimate of $g_X(z)$ is then given by the sample average $M^{-1} \sum_{i=1}^M \mathcal{K}_X(X_{z,i}, \cdot) \in \mathcal{H}_X$. Specifically, using the noise-outsourcing lemma (Theorem 6.10 of Kallenberg (2002); see also Lemma 2.1 of Zhou et al. (2022)), for any integer $m \geq 1$, there exists a measurable function \mathbb{G} such that, for any $\eta \sim N(0, I_m)$ independent of Z , we have $\mathbb{G}(\eta, Z) | Z \sim P_{X|Z}$. Based on this result, we train a generative moment matching network (GMMN, Dziugaite et al., 2015; Li et al., 2015) to approximate \mathbb{G} . For any fixed $z \in \mathbb{R}^{dz}$, we generate i.i.d. copies η_i from $N(0, I_m)$, input them into the trained GMMN $\hat{\mathbb{G}}$ along with z , and treat the outputs $\hat{\mathbb{G}}(\eta_i, z)$ as approximately sampled from the conditional distribution of X given $Z = z$. We refer to the trained GMMN as the (conditional) generator, and detailed training procedures are provided in Appendix.

In order to eliminate dependence on conditional generator estimation and improve test size accuracy, we follow Shi et al. (2021) and adopt a sample-splitting and cross-fitting framework to train the GMMN and DNN. For easy presentation, we consider two-fold splitting in this paper, although the test can be readily generalized to the multiple-fold splitting setting. Specifically, for positive integers n , M and $m \in [M]$, let $\{(X_i, Y_i, Z_i)\}_{i=1}^n$ and $\{\eta_i^m\}_{i=1}^n$ be i.i.d. copies of (X, Y, Z) and η such that $\{(X_i, Y_i, Z_i)\}_{i=1}^n, \{\eta_i^1\}_{i=1}^n, \dots, \{\eta_i^m\}_{i=1}^n$ are mutually independent. Let $\tilde{X}_i^{(m)} = \mathbb{G}(\eta_i^m, Z_i)$ denote the data sampled from $P_{X_i|Z_i}$. We divide $[n]$ into two equal folds $\mathcal{J}^{(1)}$ and $\mathcal{J}^{(2)}$ where $\mathcal{J}^{(1)} := \mathcal{J}^{(-2)} = \{1, 2, \dots, \lfloor n/2 \rfloor\}$ and $\mathcal{J}^{(2)} := \mathcal{J}^{(-1)} = [n] \setminus \mathcal{J}^{(1)}$. For $j \in [2]$, we train a GMMN generator $\hat{\mathbb{G}}_j$ using data (X_i, Z_i) for $i \in \mathcal{J}^{(-j)}$. Similarly, we train a DNN \hat{g}_j using data (Y_i, Z_i) for $i \in \mathcal{J}^{(-j)}$ as an estimator of g_Y (four neural networks are trained in total). Let $\hat{X}_i^{(m)} = \hat{\mathbb{G}}_j(\eta_i^m, Z_i)$ and $\hat{g}_Y(Z_i) = \hat{g}_j(Z_i)$ if $i \in \mathcal{J}^{(j)}$, then we define the test statistic as

$$\begin{aligned} \hat{T}_n &= \frac{1}{2} \sum_{s=1}^2 \left[\frac{1}{\frac{n}{2}(\frac{n}{2}-1)} \sum_{\substack{j \neq k \\ j, k \in \mathcal{J}^{(s)}}} \hat{U}(X_j, X_k) \hat{V}(Y_j, Y_k) \mathcal{K}_Z(Z_j, Z_k) \right], \\ \text{where } \hat{U}(X_j, X_k) &= \mathcal{K}_X(X_j, X_k) - \frac{1}{M} \sum_{m=1}^M \mathcal{K}_X(X_j, \hat{X}_k^{(m)}) \\ &\quad - \frac{1}{M} \sum_{m=1}^M \mathcal{K}_X(X_k, \hat{X}_j^{(m)}) + \frac{1}{M} \sum_{m=1}^M \mathcal{K}_X(\hat{X}_j^{(m)}, \hat{X}_k^{(m)}), \\ \text{and } \hat{V}(Y_j, Y_k) &= [Y_j - \hat{g}_Y(Z_j)]^\top [Y_k - \hat{g}_Y(Z_k)]. \end{aligned}$$

As will be shown in Theorem 6 below, the limiting null distribution of $n\hat{T}_n$ depends on the unknown distribution P_{XYZ} . Consequently, we cannot directly determine the rejection threshold

of $n\widehat{T}_n$ without knowing P_{XYZ} . Instead, we employ a wild bootstrap method to approximate the distribution of $n\widehat{T}_n$. Following Section 2.4 of Zhang et al. (2018), for a positive integer B and $b \in [B]$, we generate $\{e_{bi}\}_{i=1}^n$ from a Rademacher distribution, and define the bootstrap version of \widehat{T}_n as

$$\widehat{M}_n^b = \frac{1}{2} \sum_{s=1}^2 \left\{ \frac{1}{\frac{n}{2}(\frac{n}{2}-1)} \sum_{\substack{j \neq k \\ j, k \in \mathcal{J}^{(s)}}} \widehat{U}(X_j, X_k) \widehat{V}(Y_j, Y_k) \cdot \mathcal{K}_Z(Z_j, Z_k) e_{bj} e_{bk} \right\}. \quad (2)$$

Since $\{\widehat{M}_n^1, \widehat{M}_n^2, \dots, \widehat{M}_n^B\}$ can be viewed as samples from the distribution of \widehat{T}_n (c.f. Theorem 10), we reject H_0 at level $\gamma \in (0, 1)$ if $\frac{1}{B} \sum_{b=1}^B \mathbb{1}_{\{n\widehat{M}_n^b > n\widehat{T}_n\}} < \gamma$. As a default choice, we set $B = 1,000$ throughout our numerical experiments.

2.3 Theoretical properties

In this part, we evaluate the asymptotic performance of the test as the sample size increases, focusing on its empirical size (Type-I error) control and power against (local) alternatives. Specifically, we aim to determine whether the proposed test satisfies two desirable theoretical properties: 1. the probability of incorrectly rejecting the null hypothesis converges to the specified significance level γ as the sample size grows; 2. the test maintains the capability to detect (local) alternative hypotheses with a deviation from null that diminishes at the parametric rate of $n^{-1/2}$.

From our procedure, we define the event $\text{Rej}_n := \{B^{-1} \sum_{b=1}^B \mathbb{1}_{\{n\widehat{M}_n^b > n\widehat{T}_n\}} < \gamma\}$ as rejecting H_0 . To demonstrate that our proposed test has an accurate asymptotic size, it suffices to prove that the probability of rejecting H_0 , given that H_0 is true, converges to the specified level γ , i.e., $\lim_{n \rightarrow \infty} \mathbb{P}(\text{Rej}_n | H_0) = \gamma$. To achieve this, we first derive the limiting null distribution of $n\widehat{T}_n$ in Theorem 6. Subsequently, we show the consistency of our bootstrap procedure in Theorem 10, that is, conditional on the sample, the rescaled bootstrap statistic converges to the same limiting null distribution. To study the asymptotic power of our proposed test, we define a local alternative hypothesis in equation (4) whose deviation from null scales as $n^{-\alpha}$ for some $\alpha \geq 0$. The asymptotic behavior of \widehat{T}_n and the bootstrap counterpart under different values of α is analyzed in Theorem 9 and Theorem 10, respectively. Based on these results, we derive the asymptotic power of the test in Theorem 10. Let T_n denote the oracle test statistic, defined similarly to \widehat{T}_n , except that the estimated nuisance parameters (g_Y, g_X) are replaced with their true values; see Appendix for the precise definition.

The following assumption is needed to derive the asymptotic properties of our statistic.

Assumption 4. Assume $M \rightarrow \infty$ as $n \rightarrow \infty$. For $C_0 > 0$, $\alpha_1, \alpha_2 \in (0, \frac{1}{2})$ such that $\alpha_1 + \alpha_2 > \frac{1}{2}$, $D_i \in \{X_i, \widehat{X}_i^{(1)}, \widehat{X}_i^{(1)}\}$, $E_i \in \{Y_i, g_Y(Z_i), \widehat{g}_Y(Z_i)\}$ and $i \in \{i_1, i_2\}$ where $i_s \in \mathcal{J}^{(s)}$ for each $s \in [2]$, we have:

- (a) $\mathbb{E} \left\{ \|E_i\|_2^2 + \mathcal{K}_X(D_i, D_i) \mathcal{K}_Z(Z_i, Z_i) + \mathcal{K}_X(D_i, D_i) \|E_i\|_2^2 \mathcal{K}_Z(Z_i, Z_i) \right\} < C_0$.
- (b) $\left[\mathbb{E} \left\{ \|\mathbb{E}[\mathcal{K}_X(\cdot, X_i) | Z_i] - \mathbb{E}[\mathcal{K}_X(\cdot, \widehat{X}_i^{(1)}) | Z_i]\|_{\mathbb{H}_X}^2 [\sqrt{\mathcal{K}_Z(Z_i, Z_i)} + \|E_i\|_2^2 \mathcal{K}_Z(Z_i, Z_i)] \right\} \right]^{1/2} = O(n^{-\alpha_1})$ and $\left[\mathbb{E} \left\{ \|g_Y(Z_i) - \widehat{g}_Y(Z_i)\|_2^2 [\sqrt{\mathcal{K}_Z(Z_i, Z_i)} + \mathcal{K}_X(D_i, D_i) \mathcal{K}_Z(Z_i, Z_i)] \right\} \right]^{1/2} = O(n^{-\alpha_2})$.

Remark 5. If $\mathcal{K}_X, \mathcal{K}_Z$ are bounded kernels and $\|Y\|_2^2$ is bounded (without loss of generality, assume they are bounded by 1), then Assumption 4 reduces to $\mathbb{E}[\|\mathbb{E}[\mathcal{K}_X(\cdot, X_i) | Z_i] - \mathbb{E}[\mathcal{K}_X(\cdot, \hat{X}_i^{(1)}) | Z_i]\|_{\mathcal{H}_X}^2] = O(n^{-2\alpha_1})$ and $\mathbb{E}[\|g_Y(Z_i) - \hat{g}_Y(Z_i)\|_2^2] = O(n^{-2\alpha_2})$. Note that

$$\begin{aligned} & \mathbb{E}[\|\mathbb{E}[\mathcal{K}_X(\cdot, X_i) | Z_i] - \mathbb{E}[\mathcal{K}_X(\cdot, \hat{X}_i^{(1)}) | Z_i]\|_{\mathcal{H}_X}^2] \\ &= \mathbb{E}\left[\left\{\sup_{f \in \mathcal{H}_X: \|f\|_{\mathcal{H}_X} \leq 1} \mathbb{E}[f(\hat{X}_i^{(1)}) - f(X_i) | Z_i]\right\}^2\right] \\ &\leq \mathbb{E}\left[\left\{\sup_{f: \mathbb{R}^{d_X} \rightarrow \mathbb{R}: \|f\|_\infty \leq 1} \mathbb{E}[f(\hat{X}_i^{(1)}) - f(X_i) | Z_i]\right\}^2\right] \\ &= 2 \mathbb{E}[d_{\text{TV}}^2(P_{\hat{X}_i^{(1)}|Z_i}, P_{X_i|Z_i})], \end{aligned} \tag{3}$$

where $\|\cdot\|_\infty$ denotes the function supreme norm, and $d_{\text{TV}}(\cdot, \cdot)$ denotes the total variation distance. Here, the inequality in the second line is implied by the fact that $\|f\|_\infty = \sup_{x \in \mathbb{R}^{d_X}} |f(x)| = \sup_{x \in \mathbb{R}^{d_X}} |\langle f, \mathcal{K}_X(x, \cdot) \rangle_{\mathcal{H}_X}| \leq \|f\|_{\mathcal{H}_X} \sqrt{\mathcal{K}_X(x, x)} \leq \|f\|_{\mathcal{H}_X}$. Therefore, we can also replace the error metrics in Assumption 4 by the total variation distance and the mean squared error, i.e., $\mathbb{E}[d_{\text{TV}}^2(P_{\hat{X}_i^{(1)}|Z_i}, P_{X_i|Z_i})] = O(n^{-2\alpha_1})$ and $\mathbb{E}[\|g_Y(Z_i) - \hat{g}_Y(Z_i)\|_2^2] = O(n^{-2\alpha_2})$, which are common assumptions made in existing works for characterizing qualities of conditional generators and nonparametric regression functions. However, the total variation metric may not be a suitable metric for characterizing the closeness between nearly mutually singular distributions, which happens when data are complex objects such as images or texts exhibiting low-dimensional manifold structures (Tang and Yang, 2023).

The following theorem gives the limiting null distribution of our statistic, the proof of which is provided in Appendix.

Theorem 6. Suppose Assumptions 4 holds, then under H_0 ,

$$\hat{T}_n - T_n = O_p(n^{-1}[M^{-1/2} + n^{-\alpha_1} + n^{-\alpha_2}] + n^{-1/2-(\alpha_1+\alpha_2)})$$

and $n\hat{T}_n \xrightarrow{D} T^\dagger = T_1^\dagger + T_2^\dagger$, where $\{T_1^\dagger, T_2^\dagger\}$ are i.i.d. random variables with $T_1^\dagger = \sum_{s=1}^\infty \lambda_s(\chi_s^2 - 1)$. Here, χ_s^2 are i.i.d. chi-square random variables with one degree of freedom, and λ_s 's are eigenvalues of the compact self-adjoint operator on $L_2(\mathbb{R}^{d_X+d_Y+d_Z}, P_{XYZ})$ induced by the kernel function $h((X_1, Y_1, Z_1), (X_2, Y_2, Z_2)) = U(X_1, X_2)V(Y_1, Y_2)\mathcal{K}_Z(Z_1, Z_2)$; that is, there exists orthonormal basis $\{f_i(X_1, Y_1, Z_1)\}_{i=1}^\infty$ of $L_2(\mathbb{R}^{d_X+d_Y+d_Z}, P_{XYZ})$ such that

$$\mathbb{E}[h((X_1, Y_1, Z_1), (x, y, z))f_i(X_1, Y_1, Z_1)] = \lambda_i f_i(x, y, z).$$

From this theorem, we observe that the “plugged-in” test statistic \hat{T}_n becomes asymptotically equivalent to the oracle statistic T_n as long as $\alpha_1 + \alpha_2 > 1/2$. This demonstrates the property of *double robustness*: the slowly decaying nonparametric estimation errors in (g_Y, g_X) do not compromise the asymptotic accuracy of the test, provided the product of these errors decays faster than $n^{-1/2}$.

Now let us switch to the asymptotic power of the test under local alternatives. We use the triple (X^0, Y^0, Z^0) to denote (X, Y, Z) under H_0 and consider a sequence of triples (X^0, Y_n^A, Z^0)

under the alternative hypothesis:

$$H_{1n} : Y_n^A = \mathbb{E}[Y^0|Z^0] + n^{-\alpha}\mathcal{G}(X^0, Z^0) + \mathcal{R}_n. \quad (4)$$

Here, the \mathbb{R}^{d_Y} -valued function \mathcal{G} and the random vector \mathcal{R}_n satisfy $\mathbb{E}[\mathcal{G}(X^0, Z^0)|Z^0] = 0$ and $\mathbb{E}[\mathcal{R}_n|X^0, Z^0] = 0$, respectively, so that the exponent $\alpha \geq 0$ determines the decay rate of the deviation from null under H_{1n} ; for instance, setting $\alpha = 0$ and $\mathcal{R}_n \equiv \mathcal{R}$ corresponds to a fixed alternative. The following assumption is needed to derive the asymptotic results under H_{1n} when $\alpha > 0$.

Assumption 7. For $D \in \{\mathcal{K}_X(X^0, \cdot), g_X(Z^0)\}$, there exists a random variable $\zeta \in \mathbb{R}^{d_Y}$ such that $\mathbb{E}\left\{\|D\|_{\mathbb{H}_X}^2 \|\mathcal{R}_n - \zeta\|_2^2 \mathcal{K}_Z(Z^0, Z^0)\right\} \rightarrow 0$.

Remark 8. Assumption 7 implies that when $\alpha > 0$, the demeaned random vector $\mathcal{R}_n = Y_n^A - \mathbb{E}[Y_n^A|X^0, Z^0]$ converges to some random vector ζ . Instead of fixing $\mathcal{R}_n = Y^0 - \mathbb{E}[Y^0|Z^0]$ as in nonparametric regression models (see equation (1.1) in Zhu and Zhu (2018)), we allow \mathcal{R}_n to change with n and ζ can be different from $Y^0 - \mathbb{E}[Y^0|Z^0]$.

Theorem 9. Suppose Assumptions 4 holds, then under H_{1n} ,

1. If $\alpha = 0$, then $\sqrt{n}(\widehat{T}_n - c_0) \xrightarrow{D} \frac{1}{\sqrt{2}} \sum_{j=1}^2 \mathcal{G}_j^{(0)}$, where $c_0 = \mathbb{E}\left\{U(X_1, X_2)V(Y_1, Y_2)\mathcal{K}_Z(Z_1, Z_2)\right\} > 0$, and $\{\mathcal{G}_1^{(0)}, \mathcal{G}_2^{(0)}\}$ are i.i.d. mean zero normal random variables with variance equal to $4 \text{Var}\left(\mathbb{E}\left\{U(X_1, X_2)V(Y_1, Y_2)\mathcal{K}_Z(Z_1, Z_2) \middle| X_2, Y_2, Z_2\right\}\right)$.

With Assumption 7 further satisfied, we have

2. If $0 < \alpha < 1/2$, then $n^{2\alpha}\widehat{T}_n \xrightarrow{P} c$, where $c = \mathbb{E}\left\{U(X_1, X_2)\mathcal{G}(X_1, Z_1)^\top \mathcal{G}(X_2, Z_2)\mathcal{K}_Z(Z_1, Z_2)\right\} > 0$.
3. If $\alpha = 1/2$, then $n\widehat{T}_n \xrightarrow{D} c + T_A^\dagger + \frac{1}{\sqrt{2}} \sum_{j=1}^2 \mathcal{G}_j$, where $T_A^\dagger = \sum_{j=1}^2 T_{Aj}^\dagger$ and $\{T_{A1}^\dagger, T_{A2}^\dagger\}$ are i.i.d. random variables with $T_{A1}^\dagger = \sum_{i=1}^\infty \lambda_i^A (\chi_i^2 - 1)$, χ_i^2 are i.i.d. chi-square random variables with one degree of freedom and λ_i^A s are the eigenvalues corresponding to the kernel function $h((X_1, \zeta_1, Z_1), (X_2, \zeta_2, Z_2)) = U(X_1, X_2)\zeta_1^\top \zeta_2 \mathcal{K}_Z(Z_1, Z_2)$. Here \mathcal{G}_j are independent mean zero normal random variables, possibly correlated with T_{Aj}^\dagger , with variance equal to $4 \text{Var}\left(\mathbb{E}\left\{U(X_1, X_2)[\mathcal{G}(X_1, Z_1)^\top \zeta_2 + \mathcal{G}(X_2, Z_2)^\top \zeta_1]\mathcal{K}_Z(Z_1, Z_2) \middle| \zeta_2, X_2, Z_2\right\}\right)$.

4. If $\alpha > 1/2$, $n\widehat{T}_n \xrightarrow{D} T_A^\dagger$.

Theorem 6 establishes that rejecting H_0 if $n\widehat{T}_n$ exceeds the rejection threshold as the $(1 - \gamma)$ th quantile of the limiting distribution of T^\dagger constitutes a valid test procedure for H_0 with an asymptotic size of γ for any $\gamma \in (0, 1)$. Additionally, items 1 and 2 of Theorem 9 imply that $n\widehat{T}_n$ diverges to infinity under H_{1n} if the deviation from the null hypothesis decays slower than $n^{-1/2}$, ensuring the power of this test procedure to approach one as $n \rightarrow \infty$. Together, these properties imply the minimax-optimality of the test procedure based on the test statistic \widehat{T}_n , provided the rejection threshold can be computed. On the other hand, items 3 and 4 of Theorem 9 show that the test has trivial power in detecting alternatives that are too close to the null. This is expected, as even for a parametric linear model, a meaningful CMI test cannot detect local alternatives with deviations from the null decaying faster than the $n^{-1/2}$ parametric rate (e.g., see Section 1.1 of Lundborg et al. (2024)).

Finally, we demonstrate that our proposed test in Section 2.2 based on bootstrap eliminates the need to compute the rejection threshold, and the resulting test procedure is asymptotically indistinguishable from the optimal test based on $n\hat{T}_n$. For a generic bootstrapped statistic \widehat{M}_n^M defined according to equation (2) with $\{e_{bi}\}_{i=1}^n$ replaced by independent sample $\{e_i\}_{i=1}^n$ from standard normal distribution, we say that \widehat{M}_n^M converges in distribution in probability to a random variable B^* if, for any subsequence $\widehat{M}_{n_k}^{M_k}$, there exists a further subsequence $\widehat{M}_{n_{k_j}}^{M_{k_j}}$ such that the conditional distribution of $\widehat{M}_{n_{k_j}}^{M_{k_j}}$ given the data $\{X_i, Y_i, Z_i, \eta_i^m\}_{i,m=1}^\infty$ converges in distribution to B^* almost surely (e.g., see Definition 2.1 of Zhang et al. (2018)). We use the notation $\xrightarrow{D^*}$ to denote convergence in distribution in probability.

Theorem 10. *Suppose Assumptions 4 holds, then we have,*

1. Under H_0 , $n\widehat{M}_n^M \xrightarrow{D^*} T^\dagger$.
2. Under H_{1n} with $\alpha = 0$, $n\widehat{M}_n^M \xrightarrow{D^*} T_1 = \sum_{j=1}^2 \tilde{T}_j$, where $\{\tilde{T}_1, \tilde{T}_2\}$ are i.i.d random variables with $\tilde{T}_1 = \sum_{i=1}^\infty \gamma_i(\chi_i^2 - 1)$, χ_i^2 are i.i.d chi-square random variables with one degree of freedom and γ_i s are eigenvalues of $h((X_1, Y_1, Z_1), (X_2, Y_2, Z_2)) = U(X_1, X_2)V(Y_1, Y_2)\mathcal{K}_Z(Z_1, Z_2)$.

With Assumption 7 further satisfied, we have

3. Under H_{1n} with $\alpha > 0$, $n\widehat{M}_n^M \xrightarrow{D^*} T_A^\dagger$.

Furthermore, if we let $M_{nM,\gamma}^*$ denote the $(1 - \gamma)$ th quantile of $n\widehat{M}_n^M$ conditioning on the data, then the power (probability of detecting the alternative) of our testing procedure satisfies: if $\alpha < 1/2$, then $\mathbb{P}(n\hat{T}_n \geq M_{nM,\gamma}^*) \rightarrow 1$; if $\alpha = 1/2$, then $\mathbb{P}(n\hat{T}_n \geq M_{nM,\gamma}^*) \rightarrow \mathbb{P}(c + T_A^\dagger + \frac{1}{\sqrt{2}} \sum_{j=1}^2 \mathcal{G}_j \geq T_{0,\gamma}^A)$, where $T_{0,\gamma}^A$ denotes the $(1 - \gamma)$ th quantile of T_A^\dagger ; if $\alpha > 1/2$, then $\mathbb{P}(n\hat{T}_n \geq M_{nM,\gamma}^*) \rightarrow \gamma$.

Since $\mathbb{P}(n\hat{T}_n \geq M_{nM,\gamma}^*) = \mathbb{P}(\text{Rej}_n)$, item 1 of Theorem 10 demonstrates that the proposed test achieves asymptotically correct size; while items 2 and 3, along with the second part of the theorem, establish that the proposed test is consistent (the probability of rejecting H_0 converges to 1) when the alternative lies outside an $n^{-1/2}$ -neighborhood of H_0 (i.e., when $\alpha < 1/2$). Similar to the optimal test based on $n\hat{T}_n$ discussed after Theorem 9, the proposed test will also exhibit trivial power in detecting alternatives that are too close to the null (i.e., when $\alpha > 1/2$).

3 Simulation Results

To evaluate the finite-sample performance of our test, we adopt the two examples from Cai et al. (2024), where the response variable Y is univariate. Each experiment is repeated 500 times with sample sizes $n \in \{200, 400, 800\}$. The nominal significance level is set at 5%.

Example A1: Consider the linear regression model $Y_i = \beta_Z^\top Z_i + \beta_X^\top X_i + \epsilon_i$ for $i \in [n]$, where $\epsilon_i \stackrel{i.i.d.}{\sim} N(0, 0.5^2)$ are independent of $\{X_i, Z_i\}_{i=1}^n$, $d_X = d_Z = 25$ and $(Z_i^\top, X_i^\top) \stackrel{i.i.d.}{\sim} N(0, \Sigma)$ with the (i, j) th element of Σ being $\Sigma_{ij} = 0.3^{|i-j|}$ for $i, j \in [50]$. We set the first two components of β_Z as one and the rest as zero. For this example, the null H_0 corresponds to $\beta_X \equiv 0$. Under the sparse alternative, the first two components of β_X are $0.2/\sqrt{2}$ and the rest as zero. Under the dense alternative, every component of β_X is fixed at $0.2/\sqrt{25} = 0.04$.

Example A2: Consider the nonlinear regression model $Y_i = \beta_Z^\top Z_i + (\beta_X^\top X_i)^2 + \epsilon_i$ for $i \in [n]$, under the same β_Z and $\{X_i, Z_i, \epsilon_i\}_{i=1}^n$ as in Example A1. The null H_0 also corresponds to $\beta_X \equiv 0$. Under the sparse alternative, we set the first five components of β_X to be $10^{-1/2}$ and the rest as

Table 2: Empirical size and size adjusted power for Examples A1 and A2.

		n	pMIT XGB DNN		pMIT _e XGB DNN		pMIT _M XGB DNN		pMIT _{eM} XGB DNN		PCM	PCM _M	VIM	DSP	DSP _M	\hat{T}_n Oracle	\hat{T}_n
Example A1	H_0	200	5.6	6.4	5.8	7.0	6.2	8.4	8.0	9.6	2.0	0.0	3.2	0.0	0.0	7.0	8.8
		400	6.0	4.2	8.0	5.8	11.8	9.6	14.2	13.2	3.4	0.0	4.8	0.0	0.0	6.8	7.0
		800	7.0	11.2	9.8	12.8	14.2	17.2	20.2	21.0	1.2	0.0	4.8	0.0	0.0	7.2	5.4
	H_1 sparse	200	3.8	9.4	5.6	9.4	3.2	5.6	4.8	7.6	11.0	25.4	12.6	15.8	15.8	88.4	36.0
		400	18.6	34.6	30.4	35.8	11.8	55.2	24.8	56.8	27.0	81.8	14.8	14.8	29.8	100	98.6
		800	91.6	66.0	97.8	66.4	96.0	96.2	99.8	95.8	87.4	99.8	31.6	52.8	91.8	100	100
	H_1 dense	200	6.0	11.6	7.0	11.2	3.0	15.8	4.6	20.0	15.6	30.0	13.2	22.4	43.8	98.4	56.0
		400	17.6	63.6	32.2	65.8	11.0	83.6	20.6	86.3	29.2	87.8	17.0	47.2	76.8	100	100
		800	86.6	94.8	93.6	95.2	85.6	100	99.0	100	91.2	100	38.6	80.2	98.8	100	100
Example A2	H_0	200	5.6	6.4	5.8	7.0	6.2	8.4	8.0	9.6	2.0	0.0	3.2	0.0	0.0	7.0	8.8
		400	6.0	4.2	8.0	5.8	11.8	9.6	14.2	13.2	3.4	0.0	4.8	0.0	0.0	6.8	7.0
		800	7.0	11.2	9.8	12.8	14.2	17.2	20.2	21.0	1.2	0.0	4.8	0.0	0.0	7.2	5.4
	H_1 sparse	200	7.4	7.6	13.0	12.2	17.6	10.2	27.0	21.0	10.6	17.2	10.6	46.4	74.6	36.8	19.2
		400	27.2	24.8	47.0	29.8	28.4	50.6	57.4	60.4	23.2	82.0	26.0	73.0	90.8	80.0	76.2
		800	92.2	42.6	98.6	45.6	97.6	90.0	100	91.6	94.2	100	71.8	99.6	99.8	100	100
	H_1 dense	200	7.6	8.2	12.0	12.8	14.4	9.4	25.0	24.8	6.6	11.2	10.6	59.4	79.4	23.8	17.6
		400	14.0	32.0	27.2	36.8	15.0	67.4	33.0	75.8	13.4	43.0	12.6	84.0	96.4	57.4	57.8
		800	44.2	60.0	67.6	61.6	39.8	98.4	79.4	99.2	58.0	97.2	31.2	99.6	100	99.8	99.2

zero. Under the dense alternative, we set the first twelve components of β_X as $24^{-1/2}$ and the rest as zero.

For \hat{T}_n , we opt to use the Laplacian kernel and the bandwidth parameter for each kernel is selected according to the median heuristic (Gretton et al., 2012, Section 8). For comparison, we also include the simulation results for the CMI test proposed in (Williamson et al., 2023, Algorithm 3) (denoted as VIM), the single and multiple split statistics proposed in (Lundborg et al., 2024, Algorithm 1 and 1^{DR}) (denoted as PCM and PCM_M respectively), the single and multiple split statistics proposed in (Dai et al., 2022, equations (3) and (7)) (denoted as DSP and DSP_M respectively), the single/multiple split CMI tests proposed in Cai et al. (2024) (denoted as pMIT and pMIT_M respectively) as well as their power enhanced versions (denoted as pMIT_e and pMIT_{eM} respectively). For the four tests proposed in Cai et al. (2024), we include the simulation results when the conditional mean functions are learned using eXtreme Gradient Boosting (XGB) and DNN. In addition, we also show the simulation results for an oracle version of our statistic \hat{T}_n , where the true CME and conditional mean function of Y are used instead of their estimators.

For Example A1, as shown in Table 2, VIM and \hat{T}_n have relatively accurate size under H_0 , while PCM and DSP (as well as their multiple split versions) are severely undersized. The empirical size for pMIT with XGB estimation method is close to the nominal level, but it is oversized with DNN estimation method. The pMIT tests with multiple split and/or power enhancement all have large size distortions and the size distortion gets larger as n increases. For the size adjusted power, our test \hat{T}_n outperforms all other tests for all values of n under both sparse and dense alternatives, and VIM has the largest power loss although it also utilizes sample splitting and cross fitting. Note that pMIT_M with DNN estimation method actually has larger power than pMIT_e, which is supposed to be the power enhanced version of pMIT.

For Example A2, as shown in Table 2, the empirical size results are the same as in Example A1. For the size adjusted power, DSP and DSP_M have the best overall performances (especially when the sample size is small) and our test \hat{T}_n have similar power performance as DSP and DSP_M when $n = 800$. Note that the power performances of the tests proposed in Cai et al. (2024) depends heavily on the sparsity of the alternative and the estimation method used. The XGB estimation method has better performance under sparse alternative while the DNN estimation method outperforms under the dense alternative.

4 Imaging Data Applications

We apply our proposed CMI method to identify important facial regions for two computer vision tasks: recognizing facial expressions and predicting age.

4.1 Facial expression recognition

In this application, we examine whether covering some region of a facial image will influence the prediction accuracy of facial expression. We use the Facial Expression Recognition 2013 Dataset (FER2013, Goodfellow et al., 2013) consisting of 48×48 pixel grayscale facial images, each attached with a label from one of seven facial expressions: angry, disgust, fear, happy, sad, surprise, neutral (denoted as Expression 1-7). As in Dai et al. (2022), we consider seven cases where different hypothesized regions (HR) are covered: top left corner (TL), nose, right eye, mouth, left eye, eyes, face; see Appendix and Figure 2 for locations of these HRs.

After applying the same preprocessing procedure as outlined in Section 6.D of Dai et al. (2022), we obtain 11700 image-label pairs which will be the samples used in this application. Let $\{(X_i, Y_i)\}_{i=1}^{11700}$ denote the 48×48 pixel facial images and their corresponding labels. Note that for any $i \in [11700]$ and $j \in [7]$, $Y_i \in \mathbb{R}^7$ is an one-hot vector with the j th component being one and the rest being zero if Expression j is associated with X_i . For each HR, we use $\{Z_i\}_{i=1}^{11700}$ to denote the facial images with the HR covered in black.

The statistic \hat{T}_n is evaluated ten times on different subsamples, with sample size $n = 2000$, from the 11700 triples $\{(X_i, Y_i, Z_i)\}_{i=1}^{11700}$ and the box plot of the ten p-values are plotted in Figure 1. As comparison, we also include the p-values of the DSP_M statistics from Dai et al. (2022) with different loss functions: 0-1 loss and Cross Entropy (CE) loss. To evaluate the testing results, we calculated the test accuracy of a VGG network (Khairuddin and Chen, 2021) trained/evaluated on the whole sample $\{(Y_i, Z_i)\}_{i=1}^{11700}$, since lower accuracy indicates alternative hypothesis with stronger signal. The resulting test accuracies for different HRs, as well as the accuracy for the VGG network trained/evaluated $\{(X_i, Y_i)\}_{i=1}^{11700}$ (denoted as baseline acc), are also plotted in Figure 1; see Appendix for the sampling procedure and other implementation details.

As shown in Figure 1, the lower quantiles of the p-values from \hat{T}_n are above the 5% nominal level when nose or top left corner of the facial image is covered, indicating that these regions are not discriminative to facial expressions. For all the other HRs, the H_0 is rejected since all the p-values from \hat{T}_n are smaller than the nominal level. The test results from \hat{T}_n is consistent with the test accuracies for different HRs, since the test accuracies when nose or TL is covered are very close to the baseline acc, while for other HRs the test accuracies are noticeably lower than the baseline acc. The test results from DSP_M varies drastically when different loss functions are used. For DSP_M with 0-1 loss, the lower quantiles of the p-values are above (close to) the nominal level for the cases when left eye or both eyes are covered, whereas the test accuracies for these cases are significantly lower than baseline acc, indicating these regions are indeed important in detecting facial expressions. The DSP_M with CE loss has stronger detecting power than DSP_M with 0-1 loss since the p-values for the former is in general smaller than the p-values for the later, which means stronger . However, when TL or nose are covered (which correspond to the cases under H_0), the lower quantiles of the p-values from DSP_M with CE loss are smaller than the nominal level, which may result in inflated type-I error. In addition, the median p-values for different HRs from DSP and DSP_M do not decrease monotonously as the test accuracies decrease.

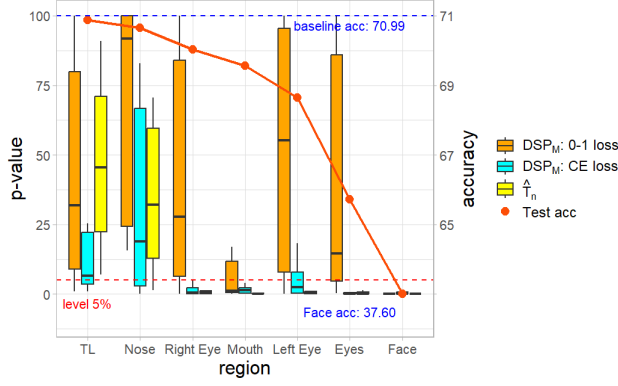


Figure 1: Box plot of the p-values (left y-axis) and the test accuracies (red line, right y-axis) for different HRs. The blue dashed line represents the baseline accuracy. The red dashed line represents the 5% nominal level. The test accuracy for the face-covered case (face acc: 37.60) is shown at the bottom right corner.

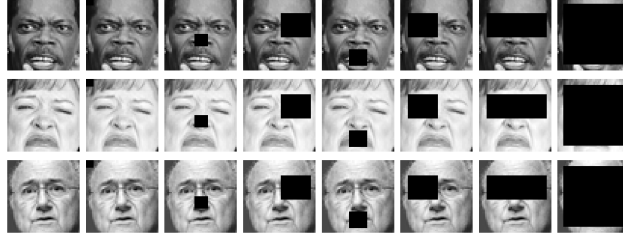


Figure 2: Original facial images in FER2013 (first column) and the covered images with HRs: TL, nose, right eye, mouth, left eye, eyes, face (Columns 2-8).

4.2 Facial age estimation

In this application, we investigate the impact of covering specific regions of facial images on the accuracy of age prediction using a well-cropped and aligned version of the UTKFace dataset (Zhang et al., 2017), which is available at <https://www.kaggle.com/datasets/abhikjha/utk-face-cropped>. We examine five scenarios where different HRs are covered: the top left corner (TL), nose, mouth, eyes, face; see Appendix and Figure 4 for the locations of these HRs.

After converting the images to grayscale and selecting the age labels ranging from 20 to 59 years old, we obtain 16425 image-label pairs, which will be the samples used in this application. Let $\{(X_i, Y_i)\}_{i=1}^{16425}$ denote the 224×224 pixel facial images and their corresponding age label $Y_i \in \mathbb{R}$. For each HR, we use $\{Z_i\}_{i=1}^{16425}$ to denote the facial images with the HR covered in black.

The statistic \hat{T}_n is evaluated ten times on different subsamples, each with a sample size of $n = 2000$, from the triples $\{(X_i, Y_i, Z_i)\}_{i=1}^{16425}$. The box plot of the ten p-values is shown in Figure 3. For comparison, we also include the p-values of the pMIT and pMIT_M statistics from Cai et al. (2024). To evaluate the testing results, we calculated the MAE (mean absolute error) of a EfficientNet B0 network (Tan and Le, 2019) trained/evaluated on the whole sample $\{(Y_i, Z_i)\}_{i=1}^{16425}$. The resulting MAE for different HRs, as well as the MAE for the EfficientNet B0 network trained/evaluated using $\{(X_i, Y_i)\}_{i=1}^{16425}$ (denoted as baseline MAE), are also plotted in Figure 1; see Appendix for the sampling procedure and other implementation details.

As shown in Figure 3, the median of the p-values from \hat{T}_n for different HRs decrease as the MAEs increase, and they are above the 5% nominal level when TL, nose, or mouth (three HRs with the smallest MAEs) of the facial image is covered, indicating that these regions are not discriminative for age estimation. For the eyes- and face-covered cases, the null hypothesis H_0 is

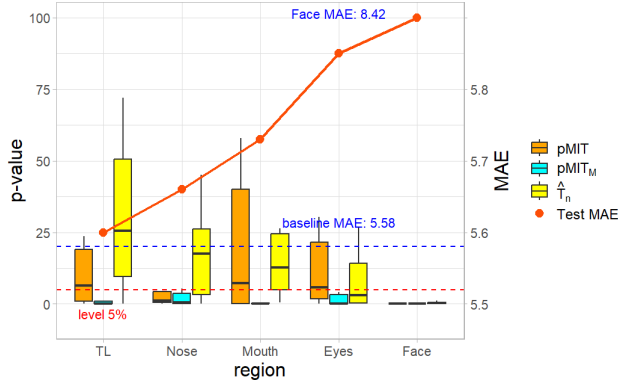


Figure 3: Box plot of the p-values (left y-axis) and the test MAE (red line, right y-axis) for different HRs. The blue dashed line represents the baseline MAE. The red dashed line represents the 5% nominal level. The test MAE for the face-covered case (face MAE: 8.42) is shown at the bottom right corner.

rejected since the median of p-values from \hat{T}_n are smaller than the nominal level, which makes sense since the test MAE in these two cases are significantly larger than the baseline MAE.

The p-values from $pMIT_M$ are all lower than the nominal level, even for the TL-covered case where the test MAE is close to the baseline MAE. This is consistent with the simulation result in Section 3 where $pMIT_M$ is severely oversized. The p-values from $pMIT$ does not change monotonously with the test MAE. Based on the median p-values, $pMIT$ rejects H_0 in the nose-covered case but failed to reject H_0 in the month- and eyes-covered cases, even though the later two have larger test MAE than the nose-covered case.



Figure 4: Original facial images in UTKFace (first column) and the covered images with HRs: TL, nose, mouth, eyes, face (Columns 2-6).

5 Conclusion

In this paper, we propose a novel conditional mean independence test that addresses limitations of existing methods. Using RKHS embedding, sample splitting, cross-fitting, and deep generative neural networks, our fully non-parametric test handles multivariate responses, performs well in high-dimensional settings, and maintains power against local alternatives converging at the $n^{-1/2}$ parametric rate. Simulations and data applications demonstrate its effectiveness. Some potential future directions include exploring conditional quantile independence testing, developing variable selection methods with false selection rate control, and performing diagnostic checks for high-dimensional regression models.

References

- Ait-Sahalia, Y., P. J. Bickel, and T. M. Stoker (2001). Goodness-of-fit tests for kernel regression with an application to option implied volatilities. *Journal of Econometrics* 105(2), 363–412.
- Bang, H. and J. M. Robins (2005). Doubly robust estimation in missing data and causal inference models. *Biometrics* 61(4), 962–973.
- Bengio, Y., A. Courville, and P. Vincent (2013). Representation learning: A review and new perspectives. *IEEE transactions on pattern analysis and machine intelligence* 35(8), 1798–1828.
- Berahmand, K., F. Daneshfar, E. S. Salehi, Y. Li, and Y. Xu (2024). Autoencoders and their applications in machine learning: a survey. *Artificial Intelligence Review* 57(2), 28.
- Cai, J., J. Luo, S. Wang, and S. Yang (2018). Feature selection in machine learning: A new perspective. *Neurocomputing* 300, 70–79.
- Cai, L., X. Guo, and W. Zhong (2024). Test and measure for partial mean dependence based on machine learning methods. *Journal of the American Statistical Association* 0(ja), 1–32.
- Cai, Z., J. Lei, and K. Roeder (2022). Model-free prediction test with application to genomics data. *Proceedings of the National Academy of Sciences* 119(34), e2205518119.
- Dai, B., X. Shen, and W. Pan (2022). Significance tests of feature relevance for a black-box learner. *IEEE transactions on neural networks and learning systems* 35(2), 1898–1911.
- Daudin, J. (1980). Partial association measures and an application to qualitative regression. *Biometrika* 67(3), 581–590.
- Delgado, M. A. and W. G. Manteiga (2001). Significance testing in nonparametric regression based on the bootstrap. *The Annals of Statistics* 29(5), 1469–1507.
- Dziugaite, G. K., D. M. Roy, and Z. Ghahramani (2015). Training generative neural networks via maximum mean discrepancy optimization. *arXiv preprint arXiv:1505.03906*.
- Fan, Y. and Q. Li (1996). Consistent model specification tests: omitted variables and semiparametric functional forms. *Econometrica: Journal of the econometric society*, 865–890.
- Goodfellow, I. J., D. Erhan, P. L. Carrier, A. Courville, M. Mirza, B. Hamner, W. Cukierski, Y. Tang, D. Thaler, D.-H. Lee, et al. (2013). Challenges in representation learning: A report on three machine learning contests. In *Neural information processing: 20th international conference, ICONIP 2013, daegu, korea, november 3-7, 2013. Proceedings, Part III* 20, pp. 117–124. Springer.
- Gretton, A., K. M. Borgwardt, M. J. Rasch, B. Schölkopf, and A. Smola (2012). A kernel two-sample test. *Journal of Machine Learning Research* 13(25), 723–773.
- Huang, J., Y. Jiao, X. Liao, J. Liu, and Z. Yu (2024). Deep dimension reduction for supervised representation learning. *IEEE Transactions on Information Theory*.
- Kallenberg, O. (2002). *Foundations of Modern Probability* (Second ed.). Springer.

- Khairuddin, Y. and Z. Chen (2021). Facial emotion recognition: State of the art performance on fer2013. *arXiv preprint arXiv:2105.03588*.
- Lavergne, P. and Q. Vuong (2000). Nonparametric significance testing. *Econometric Theory* 16(4), 576–601.
- Li, B., Y.-K. Lai, and P. L. Rosin (2017). Example-based image colorization via automatic feature selection and fusion. *Neurocomputing* 266, 687–698.
- Li, Y., K. Swersky, and R. Zemel (2015). Generative moment matching networks. In *International Conference on Machine Learning*, pp. 1718–1727.
- Lundborg, A. R. (2022). *Modern methods for variable significance testing*. Ph. D. thesis, Apollo - University of Cambridge Repository.
- Lundborg, A. R., I. Kim, R. D. Shah, and R. J. Samworth (2024). The projected covariance measure for assumption-lean variable significance testing. *The Annals of Statistics* 52(6), 2851–2878.
- Maqsood, M., F. Nazir, U. Khan, F. Aadil, H. Jamal, I. Mehmood, and O.-y. Song (2019). Transfer learning assisted classification and detection of alzheimer’s disease stages using 3d mri scans. *Sensors* 19(11), 2645.
- Murdoch, W. J., C. Singh, K. Kumbier, R. Abbasi-Asl, and B. Yu (2019). Interpretable machine learning: definitions, methods, and applications. *arXiv preprint arXiv:1901.04592*.
- Shah, R. D. and J. Peters (2020). The hardness of conditional independence testing and the generalised covariance measure. *The Annals of Statistics* 48(3), 1514–1538.
- Shi, C., T. Xu, W. Bergsma, and L. Li (2021). Double generative adversarial networks for conditional independence testing. *The Journal of Machine Learning Research* 22(1), 13029–13060.
- Song, L., J. Huang, A. Smola, and K. Fukumizu (2009). Hilbert space embeddings of conditional distributions with applications to dynamical systems. In *Proceedings of the 26th Annual International Conference on Machine Learning*, pp. 961–968.
- Szabó, Z. and B. K. Sriperumbudur (2018). Characteristic and universal tensor product kernels. *Journal of Machine Learning Research* 18(233), 1–29.
- Tan, M. and Q. Le (2019). Efficientnet: Rethinking model scaling for convolutional neural networks. In *International conference on machine learning*, pp. 6105–6114. PMLR.
- Tang, R. and Y. Yang (2023). Minimax rate of distribution estimation on unknown submanifolds under adversarial losses. *The Annals of Statistics* 51(3), 1282–1308.
- Van Landeghem, S., T. Abeel, Y. Saeys, and Y. Van de Peer (2010). Discriminative and informative features for biomolecular text mining with ensemble feature selection. *Bioinformatics* 26(18), i554–i560.
- Verdinelli, I. and L. Wasserman (2024). Feature importance: A closer look at shapley values and loco. *Statistical Science* 39(4), 623–636.

- Williamson, B. D., P. B. Gilbert, M. Carone, and N. Simon (2021). Nonparametric variable importance assessment using machine learning techniques. *Biometrics* 77(1), 9–22.
- Williamson, B. D., P. B. Gilbert, N. R. Simon, and M. Carone (2023). A general framework for inference on algorithm-agnostic variable importance. *Journal of the American Statistical Association* 118(543), 1645–1658.
- Zhang, X., S. Yao, and X. Shao (2018). Conditional mean and quantile dependence testing in high dimension. *The Annals of Statistics* 46(1), 219–246.
- Zhang, Y., L. Huang, Y. Yang, and X. Shao (2024). Doubly robust conditional independence testing with generative neural networks. *arXiv preprint arXiv:2407.17694*.
- Zhang, Z., Y. Song, and H. Qi (2017). Age progression regression by conditional adversarial autoencoder. In *Proceedings of the IEEE conference on computer vision and pattern recognition*, pp. 5810–5818.
- Zhou, X., Y. Jiao, J. Liu, and J. Huang (2022). A deep generative approach to conditional sampling. *Journal of the American Statistical Association* 118(543), 1–12.
- Zhu, X. and L. Zhu (2018). Dimension reduction-based significance testing in nonparametric regression. *Electronic Journal of Statistics* 12(1), 1468–1506.
- Zhuang, F., Z. Qi, K. Duan, D. Xi, Y. Zhu, H. Zhu, H. Xiong, and Q. He (2020). A comprehensive survey on transfer learning. *Proceedings of the IEEE* 109(1), 43–76.